IJST, Transactions of Civil Engineering, Vol. 39, No. C2, pp 283-297
Printed in The Islamic Republic of Iran, 2015

EFFECTS OF FIBER REINFORCED PLASTER ON THE EARTHQUAKE BEHAVIOR OF MASONRY BUILDINGS*

H. BAŞARAN[1], A. DEMIR[2], M. BAĞCI[3**] AND E. ERCAN[4]
[1,2,3]Dept. of Civil Engineering, Faculty of Engineering, Celal Bayar University, Manisa
Email: muhiddin.bagci@cbu.edu.tr
[4]Dept. of Civil Engineering, Faculty of Engineering, Ege University, İzmir

Abstract– In this paper the traditional covering plaster of masonry buildings is supplied with Polypropylene and steel fiber to enhance their seismic behavior. The plaster mix proportion is determined by some initial mortar tests. Also, one story, single span masonry building specimen plastered with different mortars is tested on a shaking table 8 times under a seismic input and the performance of the specimens with the above types of mortar is evaluated. The specimen plastered with a traditional plaster was regarded as control and its earthquake behavior was compared to that reinforced by fiber plaster. Steel fiber or polypropylene addition significantly increased stiffness, displacement ability and energy consumption ability of specimens as compared to control. The suggested reinforcement method was proven to strengthen masonry buildings in a fast, reliable and economical way. Moreover, it can easily be adapted to any masonry building without causing any negative impact. The suggested method is fire and corrosion resistant.

Keywords– Shake table, masonry building, fiber reinforced plaster

1. INTRODUCTION

Masonry buildings account for about 50% of all buildings in Turkey [1]. These masonry buildings, especially those built in rural areas minimally, if at all, received engineering services. Usually, people residing in these buildings have constructed them, thus these buildings do not comply with standards specified for these buildings in Turkish Earthquake Code (2007).

The horizontal loads occurring during earthquakes reveal strong planar and non-planar forces on these walls. The behaviour and the damages to these constructions under seismic forces are relatively big. The walls in the direction of the shearing force have a major role in increasing the seismic force durability. The majority of the existing buildings in this region have not been designed to withstand earthquakes. Most of them are typically unreinforced masonry, low-rise buildings and have been exiguously designed [1]. They showed poor performance during earthquakes and most of the damage and casualties resulted from these structures. However, in terms of earthquake engineering, significant lessons were learned from the surveys of damaged masonry buildings after earthquakes [1]. Damage and losses arising from landslides can include cracks in the masonry, damage to the electricity and water supply, subsidence or at worst the complete collapse of buildings [2]. Masonry building constructions constitute a significant part of the construction inheritance in the world. Actually, the structural walls of these buildings have been designed so as to resist the force of gravity. The horizontal loads incurred by earthquakes reveal strong planar and non-planar forces with these walls. The damage that occurs in these buildings under seismic forces is relatively big [2]. Figure 1 shows some pictures of masonry buildings that were damaged after the Sultandagi-Cay Earthquake, 2002.

---

*Received by the editors February 19, 2014; Accepted October 8, 2014.
**Corresponding author

Fig. 1. Damage to masonry structures

In masonry buildings, loads affecting the system were carried by inner and outer walls and were transferred to the base. Therefore, walls are of great significance in masonry buildings. Damages occurring in walls weaken the bearing system of a building. Materials used in the construction of masonry buildings such as stone and brick were bound to each other using mortar with mineral binder. Walls constructed as such are resistant to vertical loads but are not resistant to horizontal ones. To overcome this weakness, several studies have been carried out on masonry buildings and reinforcement methods for these buildings have been developed. These developed reinforcements fall into two categories. Methods in the first group are aimed to increase the adherence between the brick and mortar. To accomplish this, several additives have been put into mortar mix. Thus, strength, stiffness and ductility of masonry buildings have been reported to improve [3-12]. Studies have been carried out on numerical models related to increasing the adherence between the brick and mortar. Methods on the second group, on the other hand, have included the strengthening of brick surfaces using materials such as FRP, wires, fiber materials, steel mesh, steel and wood flat, and used tires [13-33].

In this study, a novel method in strengthening of masonry buildings was developed. Mortars used in the walls of masonry building specimens were reinforced with steel fiber and polypropylene. Mortars having the aforementioned additives improved earthquake behavior of specimens. Previous studies have used reinforcement methods on earthquake damaged buildings. However, the method used in our study can be applied to the walls of new or damaged masonry buildings.

2. MATERIALS AND METHODS

a) Material properties of specimens

The standard brick and mortar test technique for the samples prepared according to TSE 7720 [34] was used. The number of samples prepared for each of brick and mortar is 3. For the bricks that were used in the experiments, the compressive strength value was 2,65MPa, modulus of elasticity was 125MPa, and tensile strength was 0,5MPa. To optimize the grout mortar proportion was used as binder, the sand: lime: cement: water was 20/2/3,6 /1,7 [35]. The compressive strength and modulus of elasticity values obtained for the grout mortar were 2,68 and 2100 MPa, respectively, and the tensile strength value obtained from the bending test was 0,325MPa. Three types of plaster were used in the production of wall samples. These were the traditional plaster (mixture of sand, lime, mortar and water), the traditional plaster + 2% polypropylene fiber and the traditional plaster + 3% steel fiber. Plasters used in the preparation of masonry specimens are given in Table 1 [35].

Table 1. Masonry structure types

Plaster Type	Rate (% in volume)	Specimen
Normal	-	N
Polypropylene	2%	P
Steel	3%	S

A total of 24 experiments were conducted on the masonry bricks plastered with normal, polypropylene and steel fiber reinforced plasters. The wall samples were prepared with dimensions 400mmx400mm×100mm. The masonry brick walls constructed were also plastered with polypropylene and steel fiber reinforced materials under their traditional application. The plasters were applied to 10 mm thickness to the two opposite surfaces with a trowel [35]. Since the effect of the additive materials in the plastering applied was researched, the type of sand and cement used was kept fixed. Mechanical properties of masonry walls and plasters were determined with uni-axial compression test and three point bending test. Polypropylene and steel fiber additives used in plasters are shown in Fig. 2.

Fig. 2. Polypropylene and steel fiber additives used in plasters

Mechanical properties of plasters used in specimens are given in Table 2.

Table 2. The mechanical properties of mortar

Specimens	Compressive strength (Mpa)	Tensile strength (Mpa)	Elasticity modulus (MPa)
N	2.68	0.325	2100
P2	7.05	0.561	5189
S3	4.45	0.727	7917

b) Preparation of samples

For real dynamic test of scaled models on shake table, Cauchy and Froude law must be satisfied. The Cauchy law is adequate for phenomenon in which restoring forces are derived from stress-strain constitutive relationship, while Froude law applies to cases where gravity forces are important. Thus for the realistic modeling of linear dynamic response of structure both similitude laws must be satisfied, Sullivan et al. [36]. The simultaneous satisfaction of Cauchy and Froude similitude leads to scale factors represented in Table 3.

Table 3. Scale factors between prototype and model, adapted from Sullivan et al [36].

Parameter	**Symbol**	**Scale Factor**
Length	L	$L_p/L_m = \lambda$
Modulus of elasticity	E	$E_p/E_m = 1$
Specific mass	ρ	$\rho_p / \rho_m = \lambda^{-1}$
Area	A	λ^2
Volume	V	λ^3
Mass	m	λ^2
Displacement	d	λ
Velocity	v	$\lambda^{1/2}$
Acceleration	a	1
Weight	w	λ^2
Force	F	λ^2
Time	t	$\lambda^{1/2}$
Frequency	**f**	$\lambda^{-1/2}$

The acceleration scale is unity while time scale is square root of geometrical scale λ . This means that in model the time scale is compressed by a factor $\frac{1}{\sqrt{\lambda}}$. Therefore, the accelerogram applied to the structure has shorter durations, higher frequency and the same accelerations. Another important consequence of the similitude law, is the increase of the mass of the model relative to the reference prototype. To conform with the time similitude condition, time history of the original accelerogram was compressed by a factor $\frac{1}{\sqrt{3}}$. In shaking table experiments, geometric properties of one story single-span modeled masonry buildings are scaled down to one-third of real dimensions and are given in Table 4.

Table 4. Geometric properties of scaled model

Geometric properties (mm)	Real model		Scaled model		Scale
	a	b	a	b	
Building floor height	2700		900		3
Building wall thickness	300		100		3
Buildings plan size	3600	3600	1200	1200	3
Buildings window size	900	1200	300	400	3
Buildings door size	750	2250	250	750	3
Brick wall	200	100	100	50	2
Brick wall height	60		30		2

Horizontal - vertical joint gap between bricks is implemented 10 mm. Floor slabs of masonry buildings are constructed 5 cm. Horizontal bond beams supporting the slabs are 10cmx10cm. There are no lintels on the door and window openings. Window and door openings of the scaled three dimensional structure of masonry building and direction of shaking table motion are shown in Fig. 3.

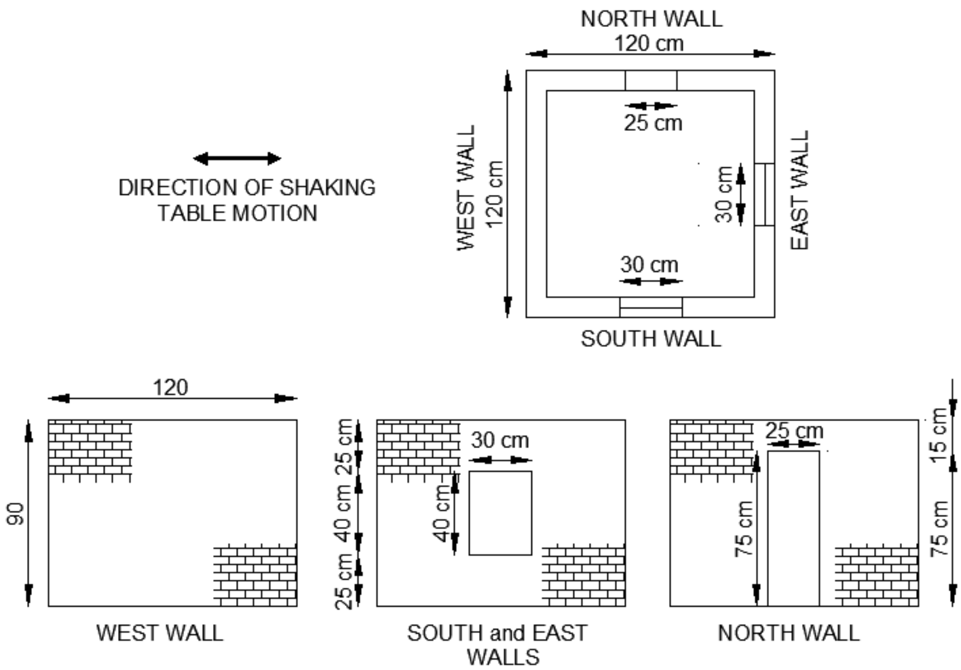

Fig. 3. Geometry of scaled three-dimensional masonry building

Brick layout used in masonry wall construction is depicted in Fig. 4.

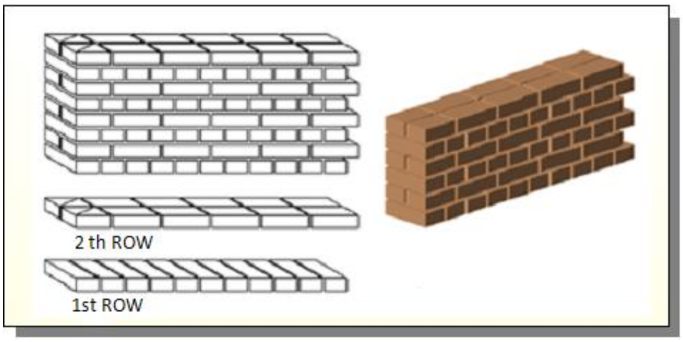

Fig. 4. Brick layout

Reinforced concrete slabs weighing 10 kN were mounted on specimens using chemical adhesives. Masonry buildings prepared in this study are shown in Fig. 5.

Fig. 5. Masonry structure specimens

c) Preparation of experimental setup

The setups of specimens are given in Fig. 6. In the shaking table tests, a table having the dimensions of 250cm x 250cm and a servo motor with a moving mechanism of 100kN horizontal force capacity and a displacement capacity of 100 cm were used. An accelerometer (biaxial ± 4 g capacity) and a 200 mm potentiometer were also used. These sensors were connected to a 32 channel-24 bit simultaneous dynamic data acquisition system.

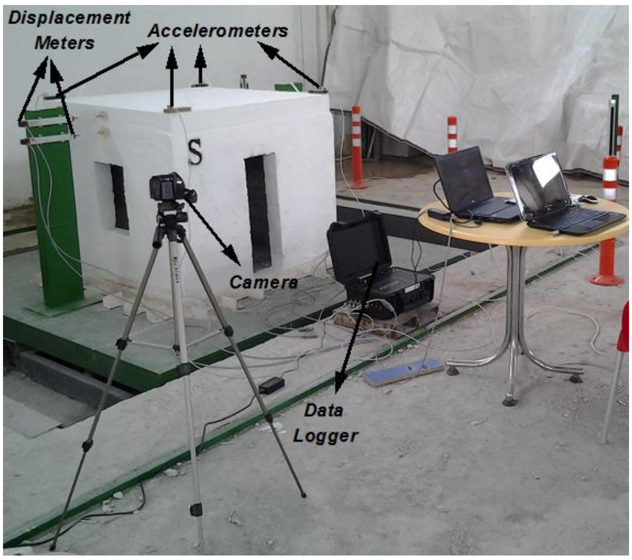

Fig. 6. Experimental setup of shaking table

The displacement meters were placed on the east and west walls as shown in Figure 3. Biaxial accelerometers were positioned on the different levels of the walls and top of the slab and one on the shaking table. Four cameras were used in the experiment. Figure 7 depicts setup diagram of the experiment.

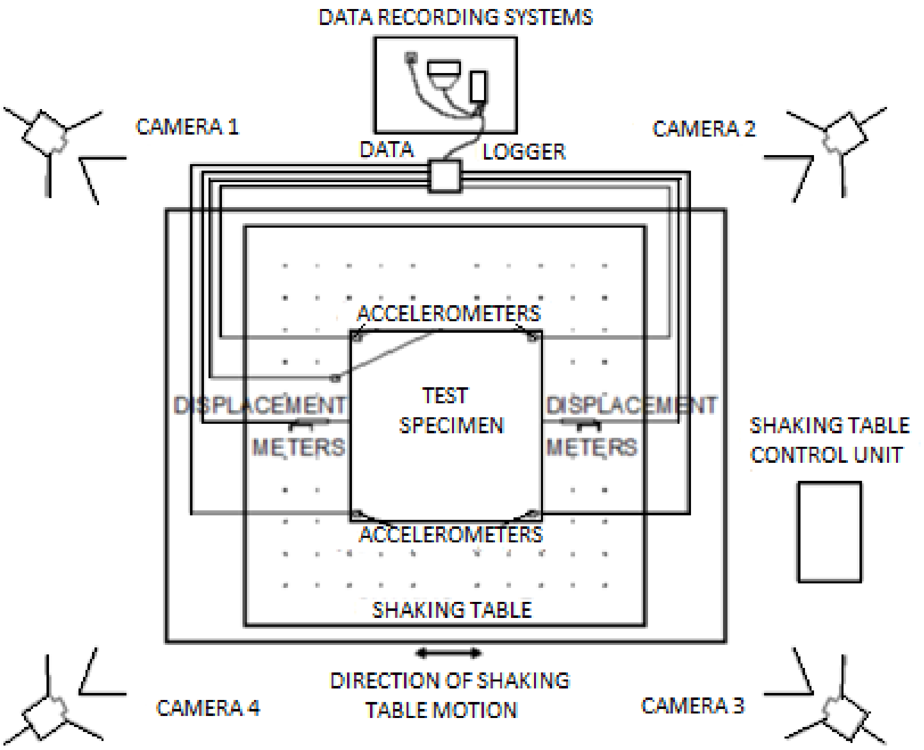

Fig. 7. Setup diagram of the experiment

To make a complete adherence between the base of the building and shaking table, chemical adhesives were used. Moreover, these regions were reinforced with steel profile. Specimens placed on the shaking table are shown in Fig. 8.

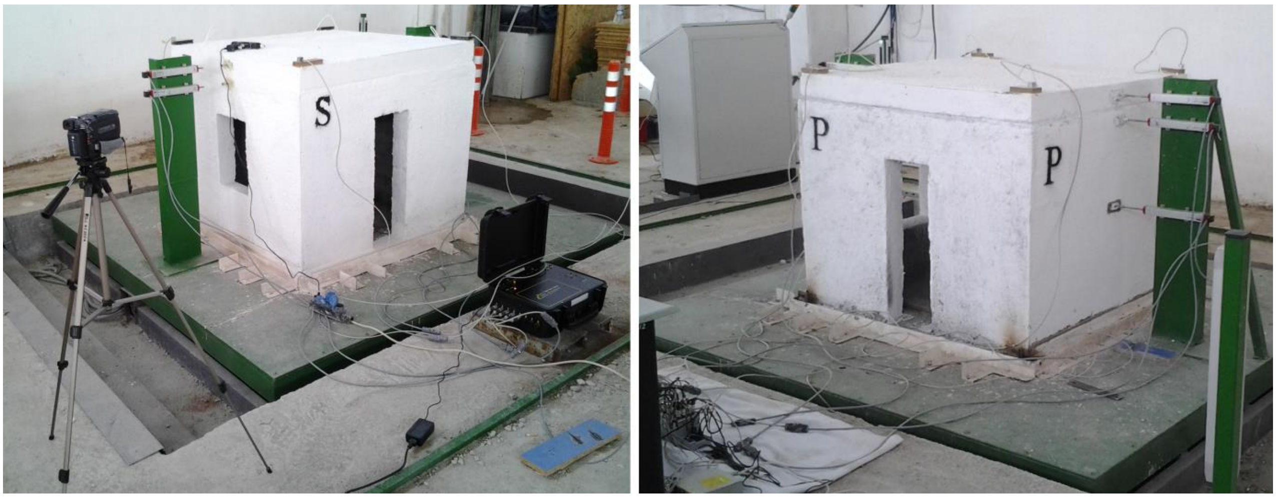

Fig. 8. Masonry buildings placed on the shaking table

d) Earthquakes

The acceleration time histories adopted for the dynamic testes were selected as strong motion record databases from the web site of Peer [37]. As stated by the EC8, the spectrum compatibility of records requires that:

- a minimum of three accelerograms should be used;
- the mean of zero period spectral acceleration values (calculated from the individual time histories) should not be smaller than the value of peak ground acceleration for the site in question;
- in the range of periods between 0,2T1 and 2T1, where T1 is the fundamental period of the structure in the direction where the accelerogram will be applied, no value of the mean 5% damping elastic spectrum, calculated from all time histories, should be less than 90% of the corresponding value of the 5% damping elastic response spectrum.

A sufficient number of ground motion records has to be used in the analyses, since it is well established that the inelastic response of structures is sensitive to the characteristics of the input motion. According to several modern seismic codes and as supported by research works [38], if the response is obtained from at least seven nonlinear time history analyses with spectrum-compatible ground motions, the average of the response quantities from all analyses should be used as design value of seismic action effect. Otherwise, the most unfavorable value of response quantity among the analyses should be used. The six real spectrum-compatible accelerograms are described in Table 5, while the records are shown in Fig. 9. They have been selected through an algorithm based on a Monte Carlo random automatic selection of the groups of accelerogram: the program automatically combines the records downloaded from the strong motion catalogues and identifies the set best reproducing the target response spectrum. The procedure is described in detail in [39].

Table 5. The acceleration time histories adopted for the dynamic tests

Earthquake	Country	Max. acceleration (g)	Max. velocity (cm/s)	Max. displacement (cm)
Düzce	Turkey	0.535	83.5	51.59
Erzincan	Turkey	0.515	83.9	27.35
Gazlı	Russia	1.264	54.2	30.15
Kocaeli	Turkey	0.376	79.5	70.52
Loma Prieta	America	0.563	94.8	41.18
Tabas	Iran	0.836	97.8	36.92
Victoria	Mexico	0.621	31.6	13.2
Westmorland	America	0.496	34.4	10.89

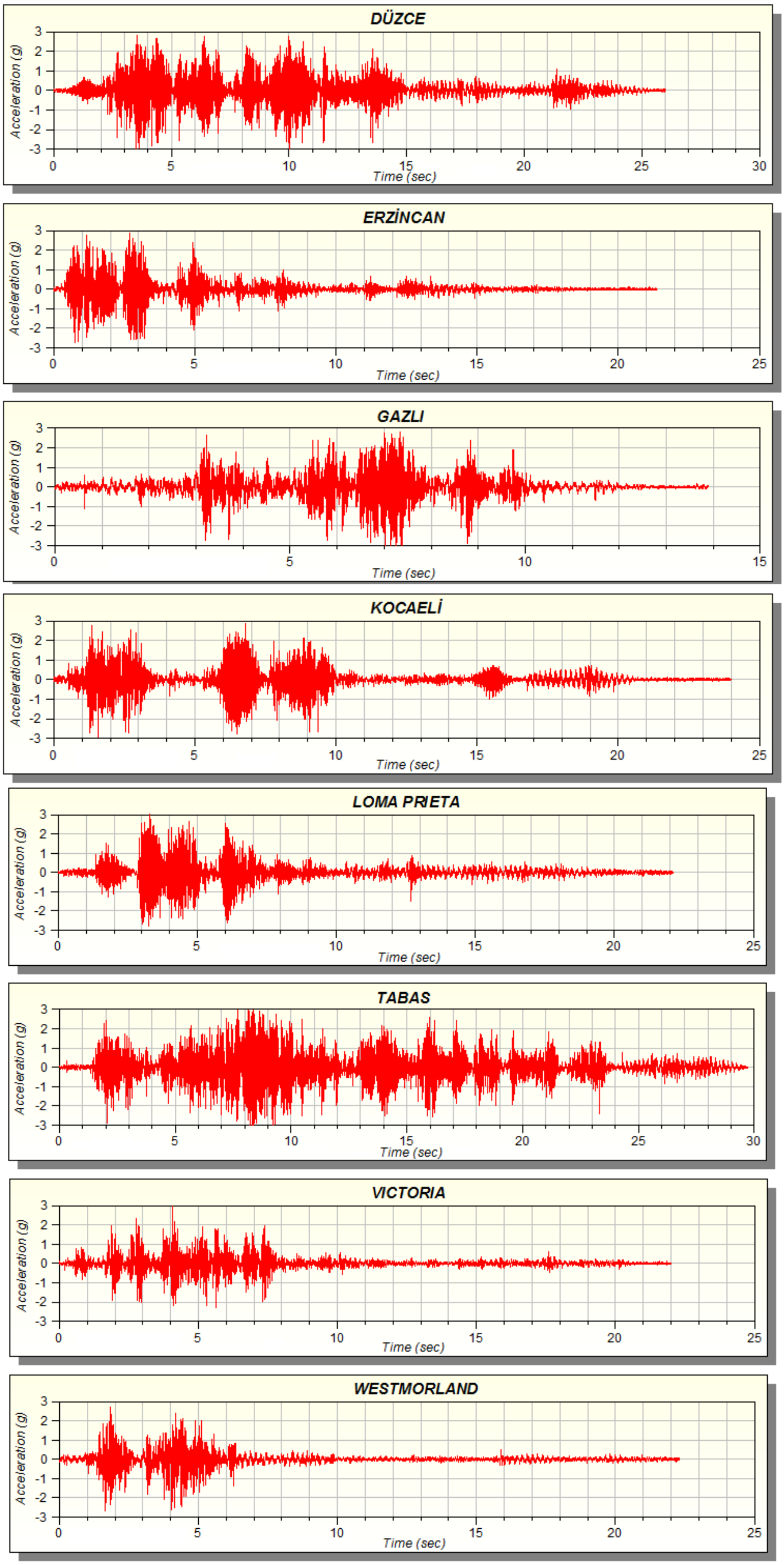

Fig. 9. Acceleration-time graphs of earthquakes on the shaking table

e) Envelope graphs

For each plastered building, envelope graphs were obtained using DIAdem software [40]. Displacement- acceleration data were recorded in every 0.01 s. The acceleration value was the arithmetic mean obtained from 4 different accelerometers. The envelope graph of Düzce earthquake is presented in Fig. 10.

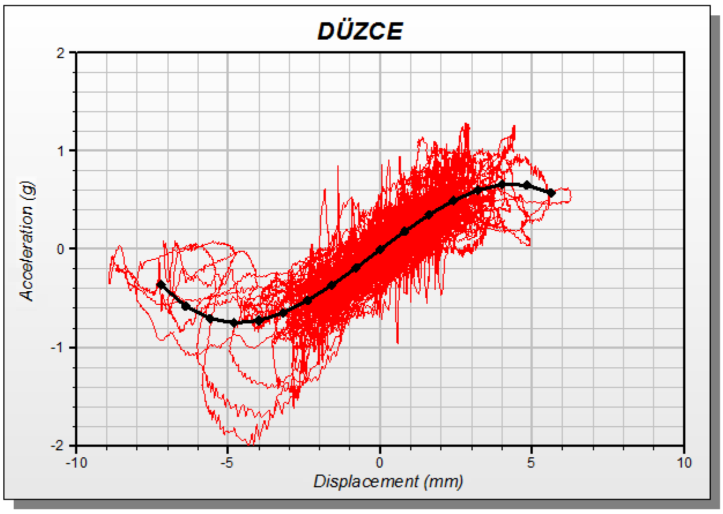

Fig. 10. Acceleration-displacement envelope graph of the normal plastered building obtained for Düzce earthquake

Similarly, envelope graphs were obtained for all earthquakes studied. Figure 11 includes envelope graphs of specimens N, P, and S.

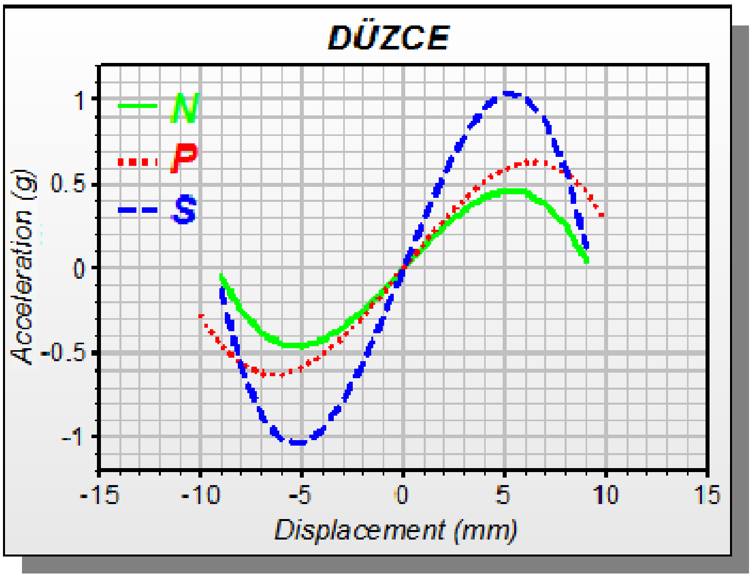

Fig. 11. Idealized acceleration-displacement envelope graph of the normal, steel and polypropylene plastered buildings obtained for Düzce earthquake

Values used in calculating displacement ability and energy dissipation capacity of specimens are depicted in Fig. 12 [35]. In this figure, ($\Delta_{0.85a_{max}}$) and ($\Delta_{0.5a_{max}}$) are displacement values corresponding to the maximum acceleration of 0.85 and 0.50.

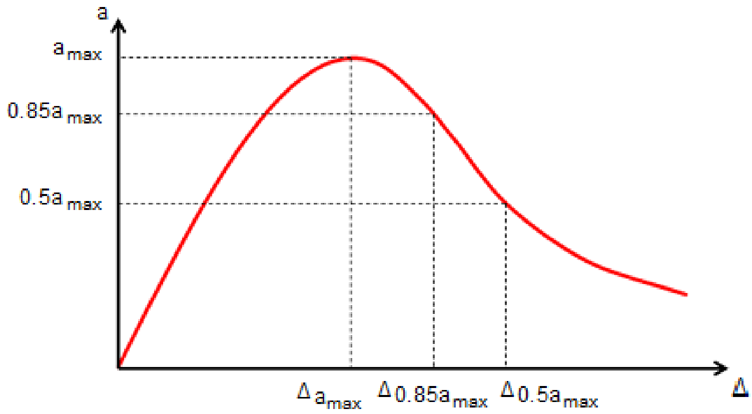

Fig. 12. Acceleration-displacement values on the envelope lines

3. RESULTS

a) Stiffness

Stiffness has been calculated as the slope of envelope graph in the linear region as shown in Figure 12. Obtained stiffness values are shown in Table 6. P and S specimens had increased stiffness values which were higher than that of N specimen. The mean increase in stiffness was 15 and 92% for specimen P and S, respectively. In reinforced plaster applications, forming of a good adherence between the wall and reinforced plaster is theorized to improve stiffness, but the displacements of stiffness specimens are lower.

Table 6. Stiffness of masonry building specimens

Earthquake	Plaster	Stiffness	Ratio of Stiffness
Düzce	N	0.12	1
	P	0.139	1.16
	S	0.282	2.35
Erzincan	N	0.185	1
	P	0.214	1.16
	S	0.314	1.7
Gazli	N	0.153	1
	P	0.175	1.14
	S	0.292	1.91
Kocaeli	N	0.12	1
	P	0.144	1.2
	S	0.276	2.3
Loma Prieta	N	0.141	1
	P	0.161	1.14
	S	0.268	1.9
Tabas	N	0.149	1
	P	0.157	1.05
	S	0.27	1.81
Victoria	N	0.171	1
	P	0.206	1.2
	S	0.315	1.84
Westmorland	N	0.186	1
	P	0.207	1.11
	S	0.295	1.59

b) Displacement ability

Displacement ability of masonry building samples was calculated using the following equations [35].

$$\mu_{a_{0.85}} = \frac{\Delta_{0.85a_{max}}}{\Delta_{a_{max}}} \tag{1}$$

$$\mu_{a_{0.5}} = \frac{\Delta_{0.5a_{max}}}{\Delta_{a_{max}}} \tag{2}$$

In the equations, $\mu_{a0.85}$ and $\mu_{a0.50}$ represent the deformation ability, and $\Delta_{0,85amax}$ and $\Delta_{0,50amax}$ represent the vertical displacement values corresponding to the 0.85 and 0.50 levels of the maximum acceleration on the decreasing arm in the acceleration -displacement curve of the relevant sample, respectively. Displacement ability of specimens is given in Table 6. Reinforced plaster application improved displacement ability (Table 7).

Table 7. Displacement ability

Earthquake	*Plaster*	a_{max}	$\Delta_{a\,max}$	$0.85a_{max}$	$0.85\Delta_{a\,max}$	$0.5a_{max}$	$0.5\Delta_{a\,max}$	$\mu_{a_{0.85}}$	$\mu_{a_{0.5}}$
Düzce	N	0.46	5.002	0.391	6.892	0.23	8.111	1.378	1.622
	P	0.628	6.041	0.533	8.332	0.314	9.883	1.379	1.636
	S	1.038	5.053	0.865	7.029	0.509	8.166	1.391	1.616
Erzincan	N	0.64	5.032	0.544	6.09	0.321	7.154	1.21	1.422
	P	0.839	5.074	0.713	7.13	0.419	8.351	1.405	1.646
	S	1.009	5.034	0.858	6.03	0.504	7.074	1.198	1.405
Gazlı	N	0.46	5.041	0.412	5.231	0.242	6.221	1.038	1.234
	P	0.812	7.012	0.691	8.562	0.406	10.175	1.221	1.451
	S	1.025	5.075	0.872	6.452	0.512	7.662	1.271	1.51
Kocaeli	N	0.403	5.061	0.342	5.921	0.201	6.932	1.17	1.37
	P	0.567	5.083	0.482	7.162	0.283	8.39	1.409	1.651
	S	0.846	4.057	0.719	5.634	0.423	6.651	1.389	1.639
Loma Prieta	N	0.551	5.015	0.468	7.125	0.275	8.341	1.421	1.663
	P	0.744	7.042	0.632	8.552	0.372	10.154	1.214	1.442
	S	0.983	5.075	0.835	6.884	0.491	8.162	1.356	1.608
Tabas	N	0.547	5.059	0.465	6.415	0.273	7.602	1.268	1.503
	P	0.818	8.042	0.695	9.804	0.409	11.512	1.219	1.431
	S	1.053	5.051	0.895	7.072	0.526	8.28	1.4	1.639
Victoria	N	0.636	5.045	0.541	6.542	0.318	7.76	1.297	1.538
	P	0.809	6.032	0.687	7.182	0.404	8.412	1.191	1.395
	S	1.096	5.012	0.932	6.415	0.548	7.59	1.28	1.514
Westmorland	N	0.694	5.064	0.59	6.552	0.347	7.781	1.294	1.537
	P	0.854	6.051	0.726	7.462	0.427	8.84	1.233	1.461
	S	1.037	5.098	0.882	6.468	0.518	7.675	1.269	1.505

c) Energy dissipation capacity

The energy dissipation capacity by each specimen has been calculated as the area beneath the envelope line as shown in Fig. 11. In the area calculation, the areas under the parts reaching the 0.85 and 0.50 levels of the maximum load level on the decreasing arm of the load-displacement curve were taken into consideration. The consumed energy value for each specimen is given in Table 8. Energy dissipation capacities of P and S specimens were compared to those of N.

Table 8. Energy dissipation capacity of masonry buildings

Earthquake	*Plaster*	$A_{a_{max}}$	$A_{0.85a_{max}}$	$A_{0.5a_{max}}$	$Ao_{a\ max}$	$Ao_{0.85a_{max}}$	$Ao_{0.5a_{max}}$
Düzce	N	1.382	2.212	2.599	1	1	1
	P	2.259	3.666	4.32	1.635	1.657	1.662
	S	3.114	5.113	5.91	2.253	2.311	2.274
Erzincan	N	2.072	2.724	3.192	1	1	1
	P	2.486	4.206	4.916	1.200	1.544	1.54
	S	3.304	4.269	4.983	1.595	1.567	1.561
Gazlı	N	1.657	1.749	2.085	1	1	1
	P	3.672	4.864	5.767	2.216	2.781	2.766
	S	3.167	4.576	5.445	1.911	2.616	2.612
Kocaeli	N	1.342	1.685	1.963	1	1	1
	P	1.676	2.857	3.342	1.249	1.696	1.702
	S	1.999	3.323	3.577	1.49	1.972	1.822
Loma Prieta	N	1.633	2.7	3.224	1	1	1
	P	3.37	4.455	5.278	2.064	1.65	1.637
	S	2.956	4.719	5.579	1.81	1.748	1.73
Tabas	N	1.696	2.426	2.883	1	1	1
	P	4.242	5.625	6.599	2.501	2.319	2.289
	S	3.133	5.225	6.106	1.847	2.154	2.118
Victoria	N	1.952	2.882	3.424	1	1	1
	P	3.197	4.089	4.781	1.638	1.419	1.396
	S	3.403	4.855	5.769	1.743	1.685	1.685
Westmorland	N	2.127	3.149	3.744	1	1	1
	P	2.416	4.086	5.257	1.136	1.298	1.404
	S	3.203	4.638	5.516	1.506	1.473	1.473

The increase in energy dissipation capacity for P, S, or N is depicted in Fig. 13.

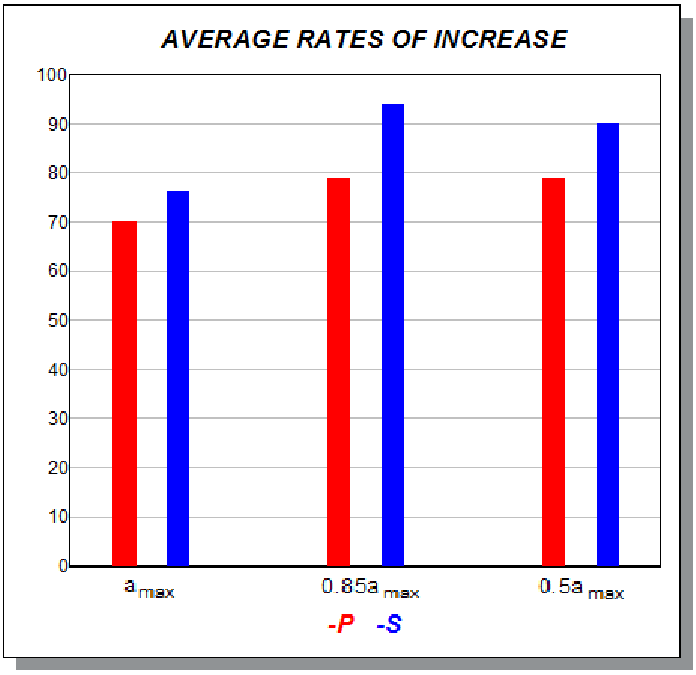

Fig. 13. Mean increase in energy dissipation capacity

In this study, in plane wall panels sliding shear called shear modes are observed on door opening after the experiment. During earthquakes, in plane walls also slide along a horizontal or stepped wall joint, a phenomenon known as sliding shear. Large out of plane displacements were observed in wall panels that failed by diagonal shear cracking. x shaped cracks are observed on out of plane wall panels are referred to as diagonal shear cracks.

4. CONCLUSION

This study addressed earthquake behavior of one story single span masonry buildings reinforced by different plasters on a shaking table. Earthquake behavior of masonry buildings reinforced by polypropylene or steel fiber was compared to that of traditionally built masonry buildings. Then, the efficacy of reinforced methods was determined calculating several parameters.

The stiffness values of masonry buildings were significantly improved by reinforcement methods used in this study. The recorded mean increase in stiffness was 15 and 92% for P and S specimens, respectively. Moreover, displacement ability and energy dissipation capacity for P or S specimens were higher than those of N. Mortars having aforementioned additives showed some positive changes on seismic behavior of specimens. It is shown that reinforcement methods used might prevent earthquake damage.

Walls reinforced by steel fiber acted as shear wall during the experiments. Fiber reinforced plaster did not de-bond from the wall and thus huge tensile stresses could be considered for preventing damages on these masonry buildings. In out of plane wall panels diagonal shear cracking was observed. In plane wall panels shear cracks were seen. Masonry buildings that suffer a shear mode of failure can be retrofitted using fiber reinforced polymer materials. The suggested reinforcement method was proven to strengthen masonry buildings in a fast, reliable and economical way. Moreover, it can easily be adapted to any masonry building without causing any negative impact. Fiber reinforced plaster is made of concrete mortar, and thus does not present any aesthetic problems. Not causing any aesthetical issues is the main advantage of our reinforcement method. Moreover, the suggested method is fire and corrosion resistant.

Acknowledgements: This study was carried out with the support of Scientific Research Coordination in Celal Bayar University within the scope of the project number 2012-47. The authors thank the institution for their support.

REFERENCES

1. Korkmaz, H. H., Korkmaz, S. Z. & Döndüren, M. S. (2010). Earthquake hazard and damage on traditional rural structures in Turkey. *Natural Hazards and Earth System Sciences*, Vol. 10, pp. 605–622.
2. Döndüren, M. S. (2008). The Effect of wall and cast mortar with improved binding property on the mechanical behaviour of out of plane loaded brick walls, *Selcuk University*, *Graduate. School of Natural and Applied Sci*. PhD Thesis, Konya.
3. Valluzzi, M. R., Binda, L. & Modena, C. (2005). Mechanical Behaviour of Historic Masonry Structures Strengthened by Bed Joints Structural Repointing, *Construction and Building Materials*, 19, pp. 63–73.
4. Emeritus, A. (2001). Masonry walls: materials and construction. *Construction and Building Materials*, Vol. 15, pp. 323-330.
5. Lucıano, R. & Sacco, E. (1998). A damage model for masonry structures. *European Journal of Mechanics, A/Solids*, Vol. 17, No. 2, pp. 285-303.
6. Laurence, P. & Rots, J. (1997). Multisurface interface model for analysis of masonry structures. *Journal of Engineering Mechanics*, Vol. 123, No. 7, pp. 660–8.
7. Lopez, J., Oller, S., Onate, E. & Lubliner, J. (1999). Homogenous constitution model for masonry, *International Journal of Numerical Mechanic Engineering*, Vol. 41, pp. 1651–1671.
8. Guinea, G. V., Hussein, G., Elices, M. & Planas, J. (2000). Micromechanical modeling of brick-masonry fracture, *Cement and Concrete Research*, Vol. 30, pp. 731–737.
9. Gabor, A., Ferrier, E., Jacquelin, E. & Hamelin, P. (2005). Analysis and modelling of the in-plane shear behaviour of hollow brick masonry panels. *Construction Building Material*, Vol. 308-321.
10. Fathy, M., Planas, J. & Sancho, M. (2008). A numerical study of masonry cracks. *Engineering Failure Analysis*, pp. 675–689.
11. Sinha, B. P., Loftus, M. D. & Temple, R. (1979). Lateral strength of model brickwork panels. *Proceedings Institution of Civil Engineers*, Vol. 67.
12. Maheri, M. R., Najafgholipour, M. A. & Rajabi, A. R. (2011). The influence of mortar head joints on the in plane and out of plane seismic strength of brick masonry walls. *Iranian Journal of Science & Technology, Transactions of Civil and Environmental Engineering*, Vol. 35, pp. 63-79.
13. Marfia, S. & Sacco, E. (2001). Modelling of reinforced masonry elements. *International Journal of Solids and Structures*, Vol. 38, pp. 4177-4198.
14. Lee, J., Pande, G., Midleton, J. & Kralj, B. (1996). Numerical modeling of brick masonry panels subject to lateral loadings, *Computer and Structure*, Vol. 61, No. 4, pp. 735–745.
15. Corradi, M., Borri, A. & Vignoli, A. (2003). Experimental study on the determination of strength of masonry walls. *Construction and Building Materials*, Vol. 17, pp. 325–337.
16. Elvin, A. & Uzoegbo, H. C. (2011). Response of a full-scale dry-stack masonry structure subject to experimentally applied earthquake loading. *Journal of the South African Institution of Civil Engineering*, Vol. 53, No. 1, pp. 22–32.
17. Griffith, M. C., Lam, N., Wilson, J. L. & Doherty, K. (2004). Experimental investigation of unreinforced brick masonry walls in flexure. *Journal of Structural Engineering, ASCE,* Vol. 130, No. 3, pp. 423–432.
18. Bayülke, N., Inan, E., Doğan, A. & Hürata, A. (1993). Impulse table tests of single story buildings. *Comprehensive Approach to Earthquake Disaster Mitigation*, pp. 183-211.

19. Magenes, G. & Calvi, G. M. (1995). Shaking table tests on brick masonry walls. *Proceedings of 10th, European Conference on Earthquake Engineering, Vienna, Austria*, Vol. 3, pp. 2419-2424.
20. Benedetti, D., Carydis, P. & Pezzoli, P. (1998). Shaking table test on 24 masonry buildings. *Earthquake Engineering and Structural Dynamics*, Vol. 27, pp. 67-90.
21. Blondet, M., Torrealva, D., Vargas, J., Velasquez, J. & Tarque, N. (2006). Seismic Reinforcement of Houses Using External Polymer Mesh. *1st European Conference of Earthquake Engineering and Seismology, Geneva-Switzerland*.
22. Karantoni, F. & Fardis, M. N. (1990). Assessment of analysis methods and of strengthening techniques for earthquake resistant masonry structures. *Structural Conservation of Stone Masonry, International Technical Conference, Rome*.
23. Gülkan, P. & Gürdil, F. (1988). Strength of Earthen Wall Subassemblies: An Experimental and Analytical Study. *Proceedings of the Ninth World Conference on Earthquake Engineering, Tokyo and Kyoto*.
24. Hendry, A.W. (2001). Masonry walls: Materials and construction. *Construction and Building Materials,* Vol. 15, pp. 323-330.
25. Krevaikas, T. D. & Triantafillou, T. C. (2005). Computer aided strengthening of masonry walls using fiber reinforced polymer strips. *Material and Structure*, Vol. 38, pp. 93–98.
26. Paulay, T. & Priestley, M. J. N. (1992). Seismic design of reinforced concrete and masonry buildings, *John Wiley & Sons Inc*.
27. Stratford, T., Pascale, G., Manfroni, O. & Bonfiglioli, B. (2004).Shear strengthening masonry panels with sheet glass-fiber reinforced polymer. *Journal of Composite Construction*, Vol. 8, No. 5, pp. 434–443.
28. Kolsch, H. (1998).Carbon fiber cement matrix (CFCM) overlay system for masonry strengthening, *Journal of Composite Construction*, Vol. 2, No. 2, pp. 105–109.
29. Ehsani, M. R., Saadatmanesh, H. & Al-Saidy, A. (1997). Shear behaviour of URM retrofitted with FRP overlays. *Journal of Composite Construction*, Vol. 1, No. 1, pp. 17–25.
30. Gabor, A., Ferrier, E., Jacquelin, E. & Hamelin, P. (2005). Modelling approaches of the in-plane shear behaviour of unreinforced and FRP strengthened masonry panels. *Composite Structures*, pp. 277–288.
31. Rosa, M. V., Valdemarca, M. & Modena, C. (2001). Behavior of brick masonry vaults strengthened by FRP laminates, *Journal of Composite Construction*.
32. Tomazevic, M. (1996). Seismic upgrading of old brick-masonry urban houses: tying of walls with steel ties. *Earthquake Spectra*, Vol. 12, No. 3, pp. 599-622.
33. Kaltakcı, M. Y., Köken, A. & Korkmaz, H. H. (2008). An experimental study on behavior of infilled steel frames under reversed cycling loading, *Iranian Journal of Science & Technology, Transactions of Civil and Environmental Engineering,* Vol. 32, pp. 157-160.
34. Turkish Standard Institute, (2000).
35. Başaran, H., Demir, A. & Bagci, M. (2013). The behavior of masonry walls with reinforced plaster mortar, *Advances in Materials Science and Engineering*, ID 436946.
36. Sullivan, T., Pinho P. & Pavese, A. (2004). An introduction to structural testing techniques in earthquake engineering, *Educational Report IUSS Press (ROSE 2004/01). Pavia, Italy*.
37. The Pacific Earthquake Engineering Research Center (PEER), University of California, Berkeley, U.S.A.
38. Bommer, J. J., Acevedo, A. B. & Douglas, J. (2003). The selection and scaling of real earthquake accelerogram for use in seismic design and assessment, *Proceedings of ACI International Conference on seismic bridge design and retrofit, La Jolla, California, U.S.A., American Concrete Institute.*
39. Dall'Ara, A., Lai, C. G. & Strobbia, C. (2006). Selection of spectrum compatible real accelerogram for seismic response analyses of soil deposits. *Proceedings of the 1st European Conference on Earthquake Engineering and seismology, Geneva, Switzerland, Paper No. 1240.*
40. DIAdem, National Instruments Ireland Resources Limited.